

AD 671553

RESEARCH REPORT
1968

THE EFFECT OF AIRDROF IMPACT ON COMPLEX STRUCTURES

by
Song Fong Jen
and
C. A. Rippe, Jr.

The University of Texas at Austin
Austin, Texas

Contract No. DAAG17-67-C-0189

December 1967



UNITED STATES ARMY
NATIONAL LABORATORIES
DURHAM, NORTH CAROLINA 27706



Microfilm edition
CLEARINGHOUSE
by U.S. Army Research Office
Durham, N.C. 27706



AIRDROF ENGINEERING LABORATORY

SECRET

This document is approved for public release and sale.
Its distribution is unlimited.

It is the policy of the Department of Defense to provide
maximum protection for our military and naval secrets.

It is the policy of the Department of Defense to provide
maximum protection for our military and naval secrets.

This document has been approved
for public release and sale; its
distribution is unlimited.

TECHNICAL REPORT
70-55-AD

THE EFFECT OF AIRDROP
IMPACT ON COMPLEX STRUCTURES

by

Song Fong Jan
E. A. Ripperger

Engineering Mechanics Research Laboratory
The University of Texas at Austin
Austin, Texas

Contract No. DAAG17-67-C-0189

Project Reference:
1M121401 D195

December 1969

Airdrop Engineering Laboratory
U. S. ARMY NATICK LABORATORIES
Natick, Massachusetts 01760

Foreword

This work was performed during the period August 1967 through December 1969 under U.S. Army Natick Laboratories Contract No. DAAG-17-67-C-0189 for the Department of the Army Project No. 1M121401 D195 entitled "Exploratory Development of Airdrop Systems" Task 13 - Impact Phenomena. The program is a part of continuing investigation directed toward obtaining improved energy dissipater materials for airdrop landing shock mitigation and a better understanding of the response of airdroppable materiel to airdrop impact phenomena.

TABLE OF CONTENTS

	<u>Page</u>
List of Figures	iv
Abstract	vi
Introduction	1
<u>Lumped Mass Model</u>	1
<u>Cushioning System Design</u>	4
Forces	4
<u>Cushioning Material Characteristics</u>	4
Design Procedure	7
<u>Analysis of the Model</u>	9
Equations of Motion	9
Element Stiffness	10
<u>Numerical Solution</u>	13
Equations	13
Digital Computer Code	15
<u>Experimental Program</u>	15
Model	15
Measurements	16
Parameter Values	16
<u>Discussion of Results</u>	18
<u>Conclusions</u>	26
<u>Recommendations for Further Studies</u>	27
<u>References</u>	28
<u>Appendix</u>	29

LIST OF FIGURES

<u>Figure</u>		<u>Page</u>
1	Laboratory Vehicle Model	2
2	Schematic of Laboratory Vehicle Model	3
3	Mathematical Model	5
4	Free Body Diagrams	6
5	Typical Stress-Strain Record for 3 in. x 3 in. x 3 in. Paper Honeycomb Samples	7
6	Idealized Cushioning System	8
7	Element Coordinates	10
8	Simple Structure Model	11
9	Element No. 1	11
10	Element No. 2	11
11	Element No. 3	12
12	Typical Deflection Gage	17
13	Measured and Computed Values of q_1 , q_5 , and q_{19} without the 3% (2.3 lb) Uncushioned Mass at q_{11} - Drop Height 18 inches	19
14	Measured and Computed Values of q_1 , q_5 , and q_{19} with 3% (2.3 lb) Uncushioned Mass at q_{11} - Drop Height 18 inches	20
15	Measured and Computed Values of Acceleration of q_5 - Drop Height 18 inches	21
16	Displacements q_1 and q_{19} without 2.3 lb (3%) Uncushioned Mass at q_{11} - Drop Height 18 inches	22
17	Displacement and Acceleration of M_3 without 2.3 lb (3%) Uncushioned Mass at q_{11} - Drop Height 18 inches	22

LIST OF FIGURES (Cont'd)

<u>Figure</u>		<u>Page</u>
18	Displacements q_1 and q_{10} with 2.3 lb (3%) Uncushioned Mass at q_{11} - Drop Height 18 inches	23
19	Displacement and Acceleration of M_3 with 2.3 lb (3%) Uncushioned Mass at q_{11} - Drop Height 18 inches	23
20	Measured and Computed Values of q_1 and q_3 without 2.3 lb (3%) Uncushioned Mass at q_{11} - Drop Height 18 inches	24
21	Main Program Flow Chart	30

ABSTRACT

The accelerations and displacements in a complex structure subjected to an impact loading are computed by treating the structure as a lumped parameter system. A mathematical model of the system consists basically of discrete masses linked by weightless, elastic beams with the appropriate stiffnesses, areas, and moment-of-inertia properties. By specifying a proper set of independent coordinates through which the motion of these lumped masses are uniquely described, and by writing equations of motion in terms of these coordinates, a set of equations is derived which represents the motion of any part of the model during impact. Using the Runge-Kutta numerical method, and a digital computer, these equations are solved.

A physical model of the lumped parameter system was built and cushioned with paper honeycomb. Displacements and accelerations at some points in this model were measured and compared with computed results. Agreement is satisfactory.

IMPACT ON COMPLEX STRUCTURES

1. Introduction

This study has two objectives; (1) to learn how to realistically model a vehicle using lumped masses and springs and to relate such computed quantities as displacement and accelerations to corresponding quantities in the prototype; and (2) to prepare a computer code for doing the necessary computations, and which is sufficiently flexible to serve as a design tool.

The report consists of eight sections as follows:

- Lumped mass model
- Cushioning system design
- Analytical study
- Numerical solution
- Digital computer code
- Experimental work
- Discussion
- Conclusion

2. Lumped Mass Model

A complex structural body can be represented by a system of discrete lumped masses connected by massless beams with appropriate flexural stiffnesses. In airdrop practice the bending moments and stresses in the structure are minimized by dividing the structure conceptually into free bodies, cushioning each part independently to provide zero rigid body rotation and equal rigid body translatory acceleration for each part. To accomplish this, the cushioning forces must be distributed over the structure in proportion to the weight.

The model shown in Figs. 1 and 2 may be regarded as a highly simplified representation of the M37 truck. The mass distribution of the truck is roughly approximated, and the various elastic beam elements simulating the structural members are assumed to have equal stiffness properties. No damping has been considered. Mass 1 can be regarded as the motor and mass 2 the load in the vehicle. Masses 3 and 4 hanging on springs below the main masses are like the wheels. Two small masses, 5 and 6, are attached in cantilever fashion to the main masses. These two do not represent anything in particular. They are included to provide information on how much such masses influence the motion of the main mass, and how the accelerations of the small masses are modified by their locations within the structure. Mass 7 (Fig. 2), which is .3% of the

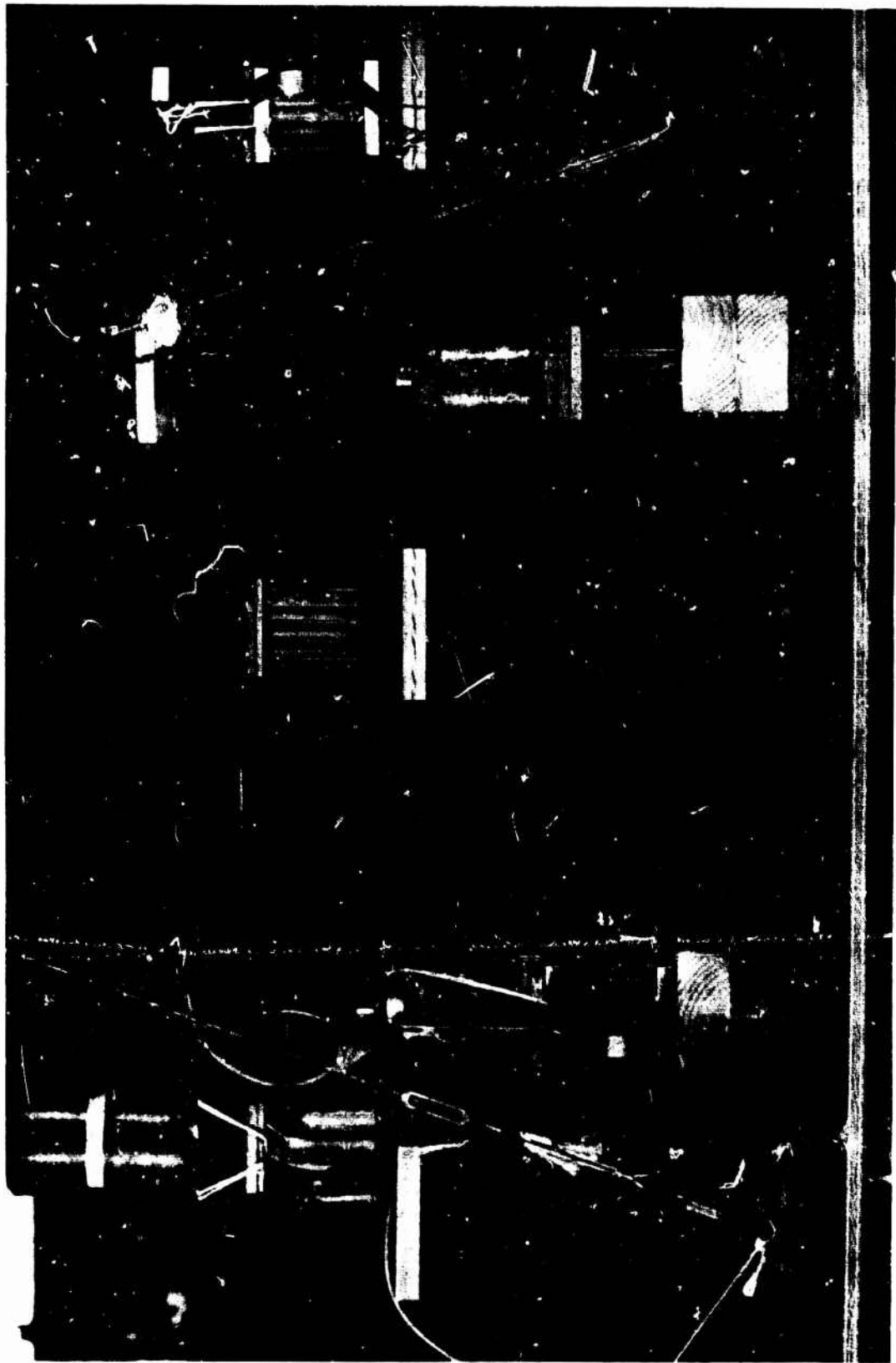


FIG. 1 LABORATORY VEHICLE MODEL

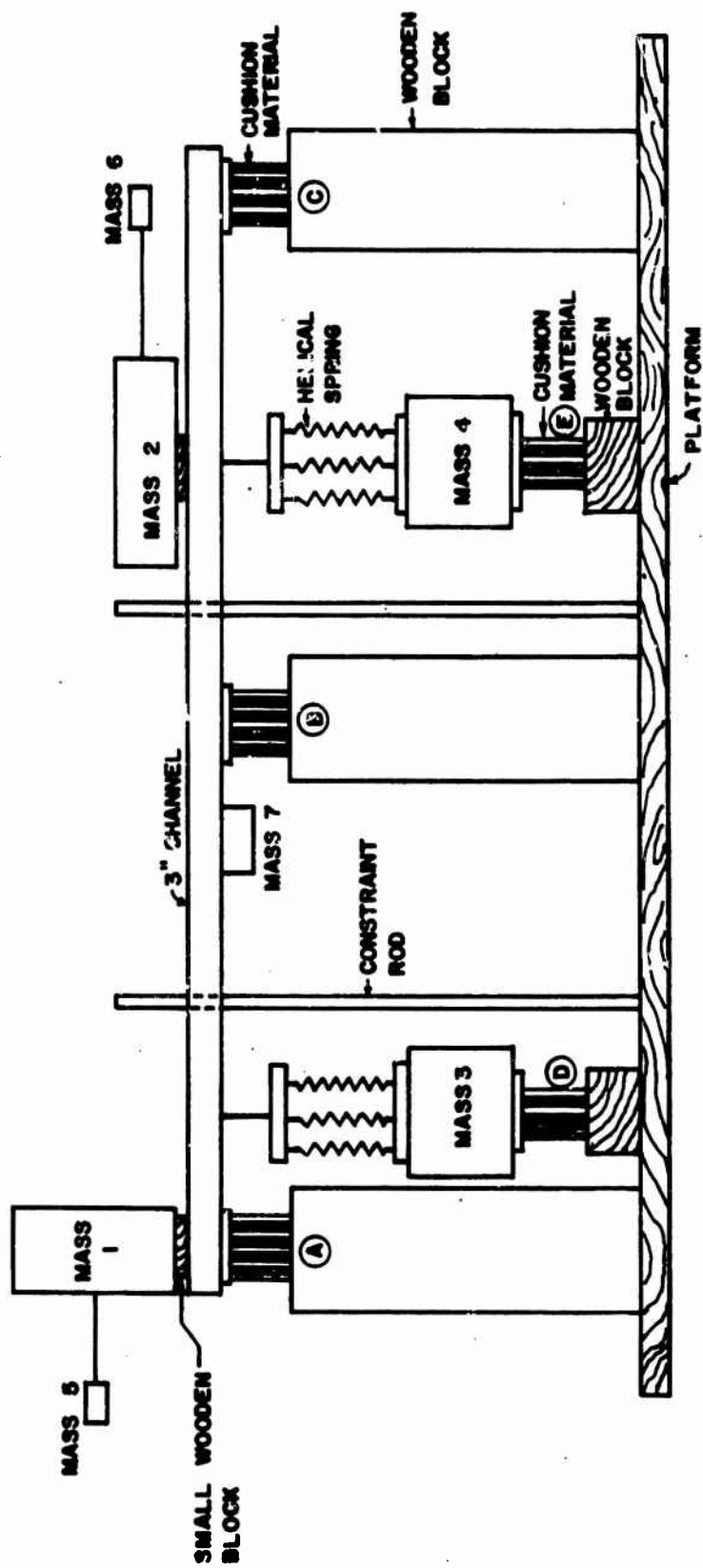


FIG. 2 SCHEMATIC OF LABORATORY VEHICLE MODEL

total model mass, has also been included to show how a small mass not attached directly to another mass may influence the motion of the main masses.

The mathematical model that corresponds to the physical model is shown in Fig. 3. If mass 7 is connected directly to the beam its very small mass in comparison with the other masses results in a large acceleration ($a = F/m$) which causes computational difficulties. To avoid these difficulties, a small beam element is used to connect this mass to the large beam.

3. Cushioning System Design

a. Forces

The overall magnitudes of the cushioning forces applied to the model as shown in Fig. 3 are determined from the acceleration level desired during impact. For a stated acceleration level of G , measured in units of acceleration of gravity, the total force applied is

$$\Sigma F = F_A + F_B + F_C + F_D + F_E = (W_1 + W_2 + W_3 + W_4) (G + 1)$$

To reduce bending moments in the long structural spans between masses, a vehicle that is to be cushioned is subdivided into free bodies, and force and moment balances are carried out for each section. Each free body has to be a statically determinate structure and no force or moment is transferred to this free body through the point of cut. If a cushioned point belongs to several free bodies then the cushioning force at that point will be the sum of cushioning forces of all free bodies at that point. For this analysis, the model has been divided into three sections. Free bodies of these three sections are shown in Fig. 4. The cushioning in the idealized mathematical model provides the forces shown.

b. Cushioning Material Characteristics

The material composing the cushioning system is idealized by assuming that it crushes at a constant strength and that it has no resilience. This is an idealization of the characteristics of paper honeycomb. The computer program at the present time includes only a constant crushing force. Time varying forces will be considered later. To obtain data applicable to the cushions used in the laboratory model nine 3 inch x 3 inch x 3 inch paper honeycomb pads were tested with a drop height of 38 inches and a mass

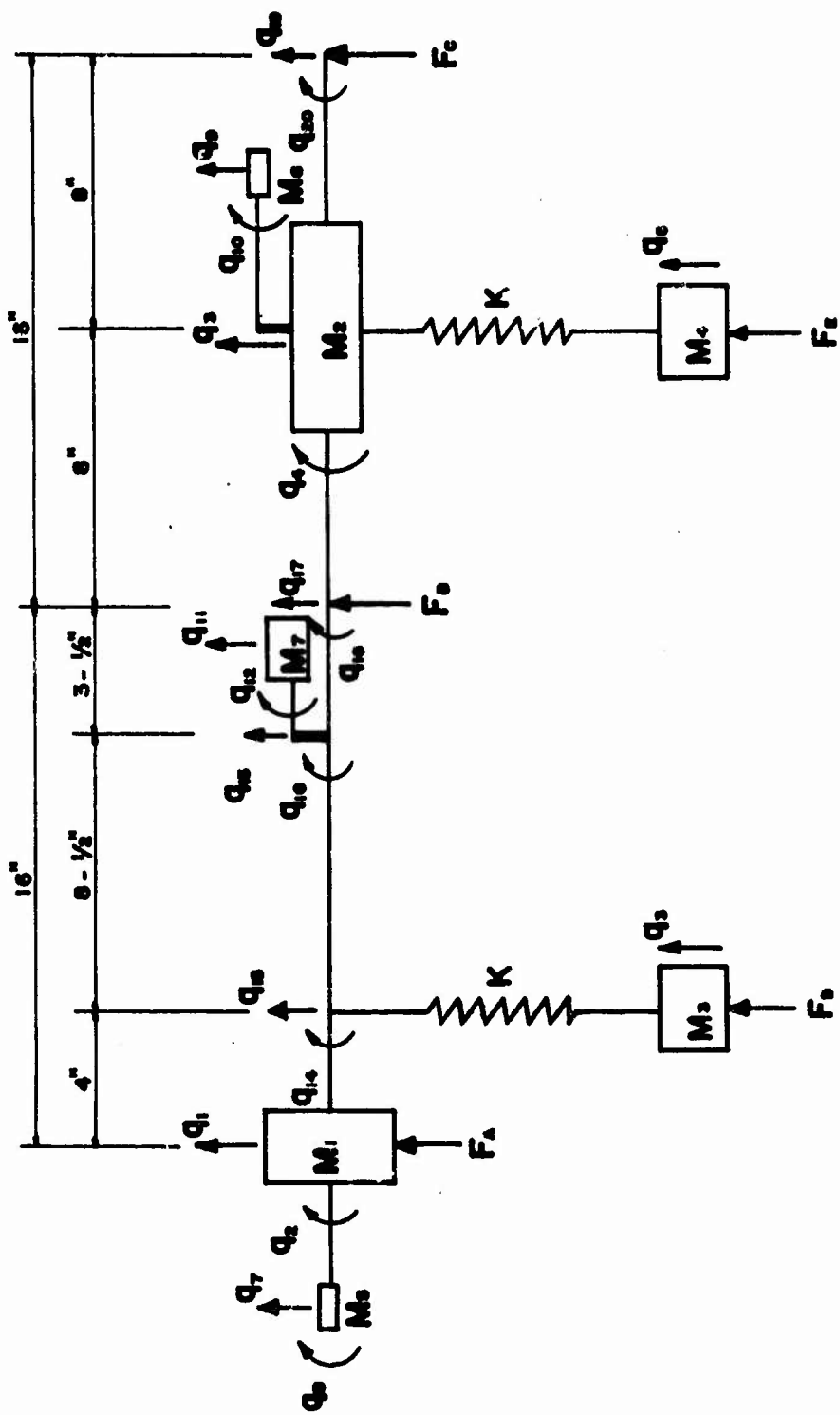
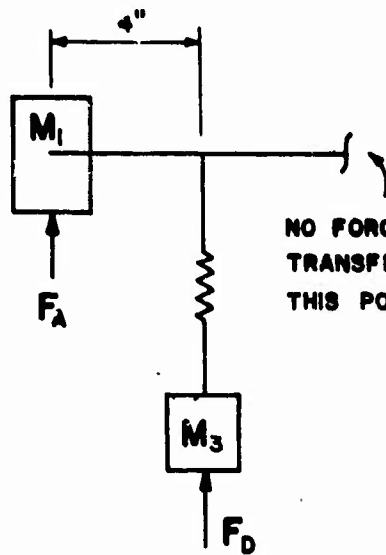


FIG. 3 MATHEMATICAL MODEL

VEHICLE SUBDIVISION

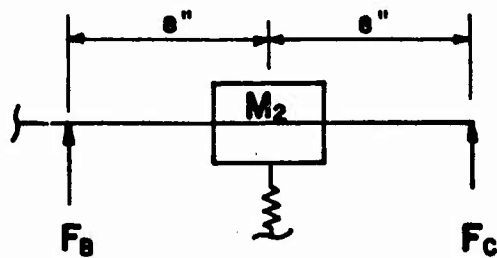
SECTION (A)



$$F_A = W_1(G+1)$$

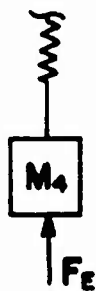
$$F_D = W_3(G+1)$$

SECTION (B)



$$F_B = F_C = \frac{1}{2} W_2(G+1)$$

SECTION (C)



$$F_E = W_4(G+1)$$

FIG. 4 FREE BODY DIAGRAMS

weight of 220 pounds. A typical stress-strain curve is shown in Fig. 5. The average strength is 4000 lb/ft². This value, due to the small size of the pad, is much smaller than the normal value for paper honeycomb (6000 psf). Based on the assumed constant crushing force of the paper honeycomb the design of the cushioning system is as follows:

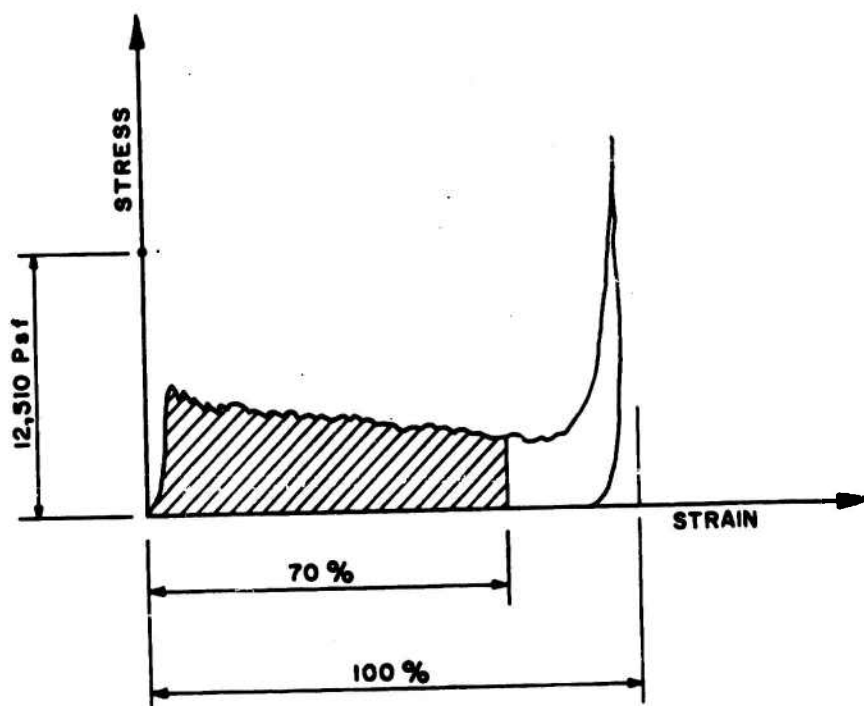


FIG. 5 TYPICAL STRESS - STRAIN RECORD FOR 3 in. X 3 in. X 3 in. PAPER HONEYCOMB SAMPLES

c. Design Procedure

First select a design acceleration level G and use Newton's law to compute cushioning force.

$$F_r = Ma \text{ -----(1)}$$

where F_r = the resultant force applied to the mass

$$M = \frac{W}{g} = \text{Mass}$$

W = weight of mass

a = acceleration of the center of gravity of the mass

$$g = 32.2 \text{ ft/sec}^2$$

Equation (1) can be rewritten as

$$F_r = WG \text{ -----(2)}$$

where $G = \frac{a}{g}$ = a dimensionless number which indicates the acceleration in "g's."

The relation between effective cushioning area A and the assumed acceleration level G , and the crushing strength S is derived as follows, referring to Fig. 6.

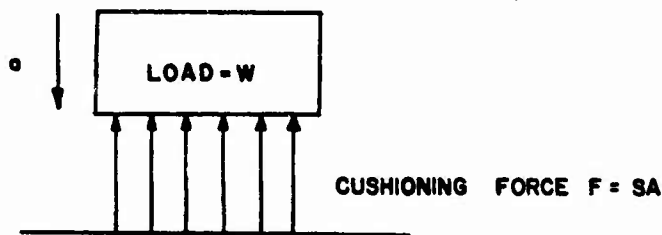


FIG. 6 IDEALIZED CUSHIONING SYSTEM

$$F - W = W\left(\frac{a}{g}\right) = WG$$

or

$$F = SA = W(G + 1)$$

and

$$A = \frac{W}{S}(G + 1) \text{ -----(3)}$$

Computation of the required thickness z of the cushion is as follows.

$$z = \frac{V}{A}$$

where V = required volume.

The volume will depend on the amount of energy to be dissipated, which will, in turn, depend on the impact velocity or the drop height h .

The potential energy U of the package will be

$$U = W(h + \epsilon z) \text{ -----(4)}$$

where

ϵ = design strain.

Since the stress-strain curve for the cushion material is assumed to be approximated by a rectangle, the amount of energy per unit volume which the pad will absorb is

$$E_n = S\epsilon \text{ -----(5)}$$

The required volume is therefore

$$V = \frac{U}{E_n} = \frac{W(h + \epsilon z)}{S\epsilon}$$

and the necessary thickness is

$$z = \frac{h}{G\epsilon} \text{ -----(6)}$$

The area and thickness of the required cushion stack thus can be obtained from Equations (3) and (6). As stated previously, the cushioning forces have been assumed constant so long as the velocity at the cushioned points remains negative, indicating downward, hence compressing movement. However, as soon as the velocity becomes zero or changes sign this cushion force will vanish.

4. Analysis of the Model

a. Equations of Motion

The general form of the equations of motion, for the model in matrix notation, is²:

$$[M]_q \{\ddot{q}\} + [K]_q \{q\} = \{Q\} \text{ -----(7)}$$

where $[M]_q$ represents the generalized mass matrix, $[K]_q$ represents the generalized stiffness matrix, and $\{Q\}$ represents the generalized force matrix. The vector $\{q\}$

represents the independent generalized coordinate system which is sufficient to uniquely describe the positions of, and the motion of the entire model, while $\{\ddot{q}\}$ is the vector describing the acceleration of the model along these coordinates. The generalized coordinates for this model are shown in Fig. 3.

b. Element Stiffness

The stiffness matrix for the individual elements is determined from elementary beam deflection theory and the equations representing the elastic force-deflection properties of the elements are combined in the following matrix expression.

$$\{F\} = [K] \{u\}$$

where

$\{F\}$ = Force vector

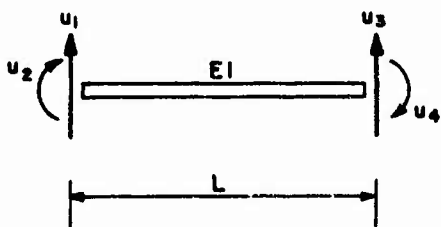
$[K]$ = Stiffness matrix

$\{u\}$ = Displacement vector

The coordinates of a beam element and a spring element are shown in Fig. 7.

The stiffness matrix for the spring element is

$$[K]_{\text{spring}} = \begin{bmatrix} k & -k \\ -k & k \end{bmatrix}$$



(a) BEAM ELEMENT



(b) SPRING ELEMENT

FIG. 7 ELEMENT COORDINATES

The element stiffness matrix for the beam is

$$[K]_{\text{beam}} = \frac{EI}{L^3} \begin{bmatrix} 12 & -6L & -12 & -6L \\ -6L & 4L^2 & 6L & 2L^2 \\ -12 & 6L & 12 & 6L \\ -6L & 2L^2 & 6L & 4L^2 \end{bmatrix}$$

The generalized stiffness matrix $[K]_0$ of the structure can be generated by synthesis from all elements of the stiffness matrix. For example, consider the simple structure in Fig. 8 and the structural element in Fig. 9. The stiffness matrix for the element is $[K]_1$

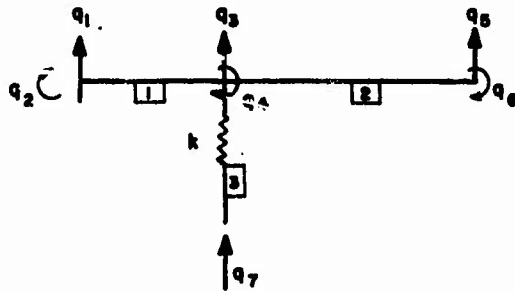


FIG. 8 SIMPLE STRUCTURE MODEL

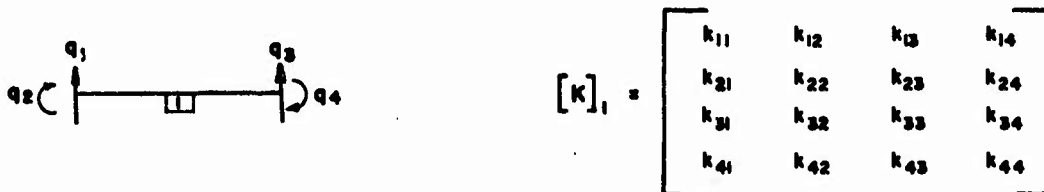


FIG. 9 ELEMENT NO. 1

where k_{11} denotes the force at coordinate q_1 when a unit load is applied at coordinate q_1 . Elements 2 and 3 and the corresponding stiffness matrices are shown in Fig. 10 and 11.

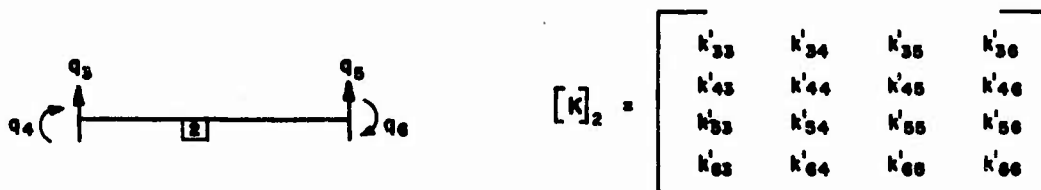


FIG. 10 ELEMENT NO. 2



$$[K]_3 = \begin{bmatrix} k''_{33} & k''_{37} \\ k''_{73} & k''_{77} \end{bmatrix}$$

FIG. 11 ELEMENT NO. 3

Then the generalized stiffness matrix is:

$$[K]_q = \begin{bmatrix} k_{11} & k_{12} & & k_{13} & & k_{14} & 0 & 0 & 0 \\ k_{21} & k_{22} & & k_{23} & & k_{24} & 0 & 0 & 0 \\ k_{31} & k_{32} & (k_{33} + k'_{33} + k''_{33}) & (k_{34} + k'_{34}) & k'_{35} & k'_{36} & k''_{37} & & \\ k_{41} & k_{42} & (k_{43} + k'_{43}) & (k_{44} + k'_{44}) & k'_{45} & k'_{46} & 0 & & \\ 0 & 0 & & k'_{53} & k'_{54} & k'_{55} & k'_{56} & 0 & \\ 0 & 0 & & k'_{63} & k'_{64} & k'_{65} & k'_{66} & 0 & \\ 0 & 0 & & k''_{73} & 0 & 0 & 0 & k''_{77} & \end{bmatrix}$$

In most situations some coordinates are required to define displacements for which there are no associated masses. Obviously, the computational acceleration $a = F/m$ will become infinite if m vanishes. To avoid this unreasonable result, the number of generalized coordinates must be reduced to the same number as the number of masses in the structure.

First it is necessary to distinguish between those displacements in $\{q\}$ associated with the masses and those associated with zero masses. Thus,

$$\{q\} = \begin{Bmatrix} \{q\}^* \\ \{q\}^0 \end{Bmatrix}$$

where

$\{q\}^*$ = displacements for which masses $[M]^*$ exist

$\{q\}^0$ = displacements for which masses are zero

The equations of motion, Equation (7), are now rewritten using the above notation.

$$\begin{bmatrix} [M]^* & | & 0 \\ \hline 0 & | & 0 \end{bmatrix} \begin{Bmatrix} \{q\}^* \\ \{q\}^0 \end{Bmatrix} + \begin{bmatrix} [K]_{11} & | & [K]_{12} \\ \hline [K]_{21} & | & [K]_{22} \end{bmatrix} \begin{Bmatrix} \{q\}^* \\ \{q\}^0 \end{Bmatrix} = \begin{Bmatrix} \{Q\}^* \\ \{Q\}^0 \end{Bmatrix} \quad (8)$$

This equation is equivalent to the two following equations.

$$[M]^*\{q\}^* + [K]_{11}\{q\}^* + [K]_{12}\{q\}^0 = \{Q\}^* \quad (9)$$

$$[K]_{21}\{q\}^* + [K]_{22}\{q\}^0 = \{Q\}^0 \quad (10)$$

The second of these equations is solved for $\{q\}^0$

$$\{q\}^0 = [K]_{22}^{-1} (\{Q\}^0 - [K]_{21}\{q\}^*) \quad (11)$$

Substituting $\{q\}^0$ into Equation (9) gives the reduced form

$$[M]^*\{q\}^* + [K]_s\{q\}^* = \{F\} \quad (12)$$

where

$$[K]_s = [K]_{11} - [K]_{12}[K]_{22}^{-1}[K]_{21} \quad (13)$$

$$\{F\} = \{Q\}^* - [K]_{12}[K]_{22}^{-1}\{Q\}^0 \quad (14)$$

Now Equation (12) can be treated to get the displacements $\{q\}^*$ of the masses. The displacements $\{q\}^*$ are then substituted into Equation (11) to obtain the displacements $\{q\}^0$ for which the masses are zero.

5. Numerical Solution

a. Equations

The equations of motion are:

$$[M]^*\{q\}^* + [K]_s\{q\}^* = \{F\} \quad (15)$$

This is a system of second order differential equations. These equations may be replaced by a system of first order equations. As a simple example, the second order equation

$$\frac{d^2y}{dt^2} = f(t, y, \frac{dy}{dt})$$

becomes the system

$$\frac{dy}{dt} = v$$

$$\frac{dv}{dt} = f(t, y, v)$$

The two functions $y(t)$ and $v(t)$ are now computed simultaneously. Initial conditions such as $y|_{t=t_0} = y_0$, $\frac{dy}{dt}|_{t=t_0} = v_0$ become $y|_{t=t_0} = y_0$, $v|_{t=t_0} = v_0$ so that

the generalized initial value problem is established.

After the equations of motion are reduced to first order differential equations, the Runge-Kutta procedure can be used to solve them. The Runge-Kutta method is briefly discussed as follows³:

Let the equations be

$$y' = f_1(t, y, v), \quad v' = f_2(t, y, v)$$

where

$$y' = \frac{dy}{dt}, \quad y = y(t), \quad v = v(t), \quad v' = \frac{dv}{dt}$$

The formulas

$$k_1 = hf_1(t_n, y_n, v_n)$$

$$L_1 = hf_2(t_n, y_n, v_n)$$

$$k_2 = hf_1(t_n + \frac{1}{2}h, y_n + \frac{1}{2}k_1, v_n + \frac{1}{2}L_1)$$

$$L_2 = hf_2(t_n + \frac{1}{2}h, y_n + \frac{1}{2}k_1, v_n + \frac{1}{2}L_1)$$

$$k_3 = hf_1(t_n + \frac{1}{2}h, y_n + \frac{1}{2}k_2, v_n + \frac{1}{2}L_2)$$

$$L_3 = hf_2(t_n + \frac{1}{2}h, y_n + \frac{1}{2}k_2, v_n + \frac{1}{2}L_2)$$

$$k_4 = hf_1(t_n + h, y_n + k_3, v_n + L_3)$$

$$L_4 = hf_2(t_n + h, y_n + k_3, v_n + L_3)$$

$$y_{n+1} = y_n + \frac{1}{6}(k_1 + 2k_2 + 2k_3 + k_4)$$

$$v_{n+1} = v_n + \frac{1}{6}(L_1 + 2L_2 + 2L_3 + L_4)$$

where $h =$ step size

may be shown to duplicate the Taylor series for both functions up through terms of order four. For more than two simultaneous equations, say n , the extension of the Runge-Kutta method parallels the above, with n sets of formulas required instead of two.

b. Digital Computer Code

A computer program code has been developed to solve the drop impact problem. This program is listed in the appendix. Only the lumped masses, cushioning forces, initial displacement and velocity and member properties such as flexural rigidity EI , spring constant k and member length L are required for input data. The computer program automatically generates the stiffness matrix of the structure and then solves the equations of motion by the Runge-Kutta method. The displacement, velocity and acceleration at any coordinate at any time may be printed out. The printed out displacement is relative to the position where impact begins. From these displacements the relative displacement of any two points can be computed. The computer code is sufficiently flexible to serve as a design tool.

6. Experimental Program

a. Model

To evaluate the computational procedure a small model has been prepared and used for collecting experimental data. This model which is shown in Fig. 1 was designed so it would be relatively simple to represent with a lumped parameter system and at the same time to have at least 10 degrees of freedom. The schematic drawing of the model shown in Fig. 2 suggests how it should be represented by lumped parameters and Fig. 3 shows the coordinates and the degrees of freedom. As indicated previously the model can be thought of as representing an M37 truck, although it was not designed specifically for that purpose. Its primary purpose is to provide a specific and convenient structure for use in evaluating the procedure developed and previously described, for computing structural response to impulsive loading.

The cushioning system for this model was designed to provide zero bending moment at the center of mass of the model. All cushioning forces are directly applied to the masses except forces F_B and F_C which are applied to the structure tied to mass 2. This loading is similar

to that applied to the M37 truck, since the dead load in the bed of the truck is not usually cushioned directly, but is cushioned through the structural members that support it. Small masses 5 and 6 are attached to the main masses 1 and 2 respectively and are cushioned. Mass 7 is optional and not cushioned.

Only vertical motion is considered. This is an oversimplification of the real situation because non-vertical motion is always possible due to wind drift and system oscillation. However, since the vertical motion is the most important factor in airdrop cushioning, it is essential that it be analyzed separately, and well understood before attempting a solution of the more general problem. Lateral and longitudinal motions of the model are minimized by the two vertical steel restraining rods, which can be seen in Fig. 1. Stability of the model is also improved by using clusters of 3 parallel springs instead of one helical spring for the support of masses 3 and 4.

b. Measurements

Accelerations are measured with fluid damped resistance type accelerometers mounted on masses 1, 2, and 3. Displacements are measured at supports A, C, and D.

To measure the deflections a special device* is used. This device which is shown in Fig. 12 consists of two U-shaped thin steel springs with strain gages mounted as shown. The legs of the U-shaped pieces can be deflected toward each other a considerable amount without the development of appreciable force or stress, and the strain gage output is proportional to the deflection. Other better known transducer types could not be used because even the small lateral motion that sometimes occurs might damage the transducer.

c. Parameter Values

Numerical values for the model parameters are

$$M_1 = 20 \text{ lb}$$

$$M_2 = 30 \text{ lb}$$

$$M_3 = M_4 = 10 \text{ lb}$$

$$M_5 = M_6 = 0.6 \text{ lb}$$

$$M_7 = 2.3 \text{ lb}$$

* Designed and developed by Dr. C. H. Yew, The University of Texas at Austin.

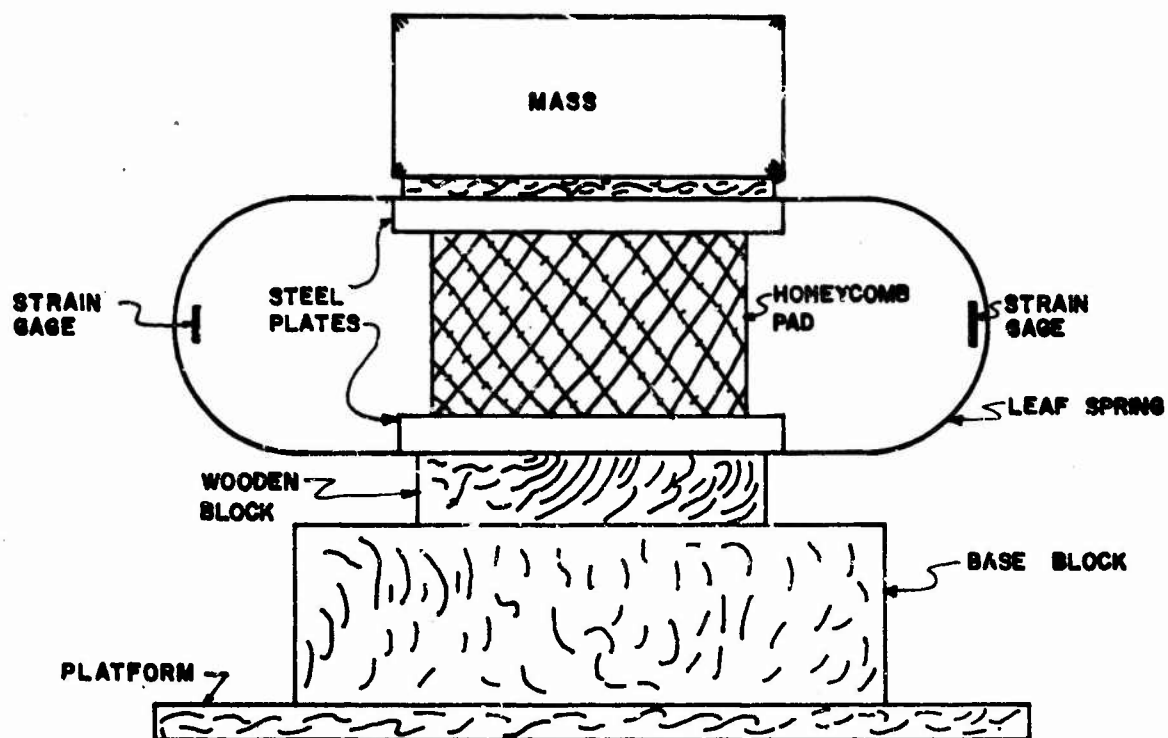


FIG. 12 TYPICAL DEFLECTION GAGE

$$K = 600 \text{ lb/in.}$$

$$E = 29 \times 10^6 \text{ psi (steel beam)}$$

$$I = 0.3393 \text{ in.}^4$$

$$F_A = 247.0 \text{ lb}$$

$$F_B = F_C = 183.5 \text{ lb}$$

$$F_D = F_E = 120 \text{ lb}$$

$$J_1 = 2.0 \text{ lb-in.-sec}^2$$

$$J_2 = 2.0 \text{ lb-in.-sec}^2$$

Paper honeycomb pad sizes are

$$A = 3 \times 2\frac{7}{8} \times 3 \text{ inches}$$

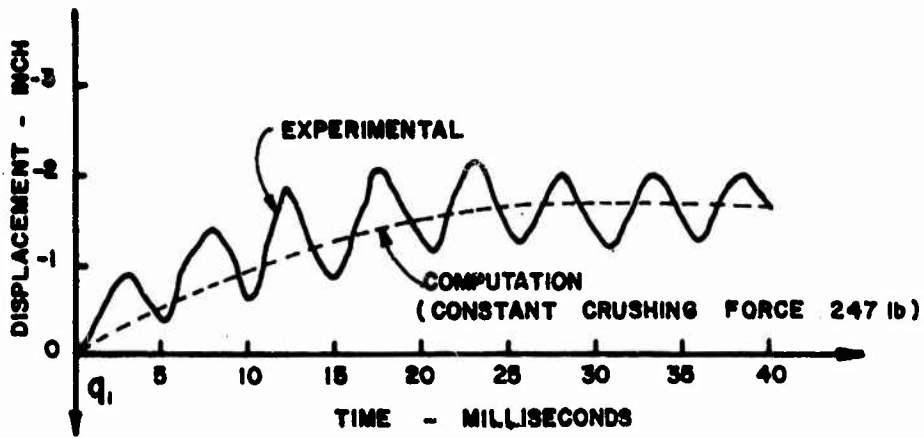
$$B = C = 2\frac{1}{2} \times 2\frac{5}{8} \times 3 \text{ inches}$$

$$D = E = 2 \times 2\frac{1}{8} \times 3 \text{ inches}$$

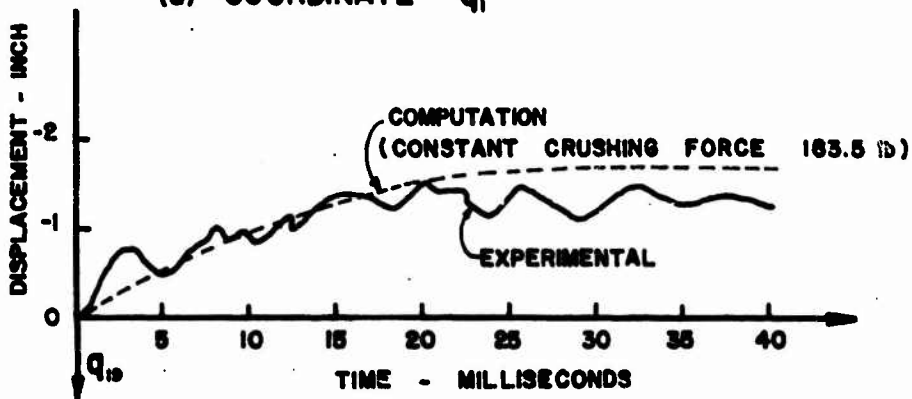
The pad sizes are selected to provide an acceleration of 12g, assuming a crushing strength of 4,000 psf for the honeycomb. This crushing strength was determined experimentally by making dynamic loading tests on samples having approximately the dimensions of these pads.

7. Discussion of Results

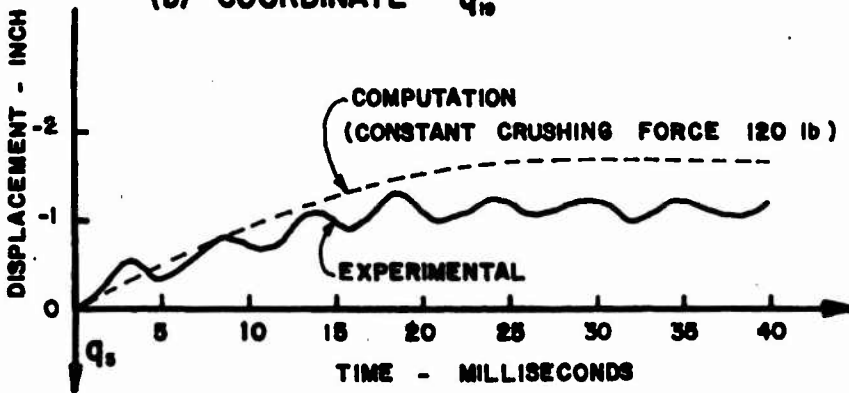
The most recent measured and computed results are shown in Figs. 13 through 20. In comparing these results it should be noted that there is a difference of some significance between the cushioning forces in the mathematical model and in the laboratory model. For the former force is assumed constant from the moment of impact until it vanishes at the instant the velocity of the cushioned mass vanishes, and from that time on it remains at zero. On the other hand the cushioning force in the laboratory model has a modest initial spike and then decreases constantly until the velocity of the cushioned mass vanishes. At that time, which incidentally does not coincide with the time the corresponding velocity in the mathematical model vanishes, the force does not drop immediately to zero because the cushion has some resiliency. The differences in the crushing forces are reflected by differences in the accelerations shown in



(a) COORDINATE q_1

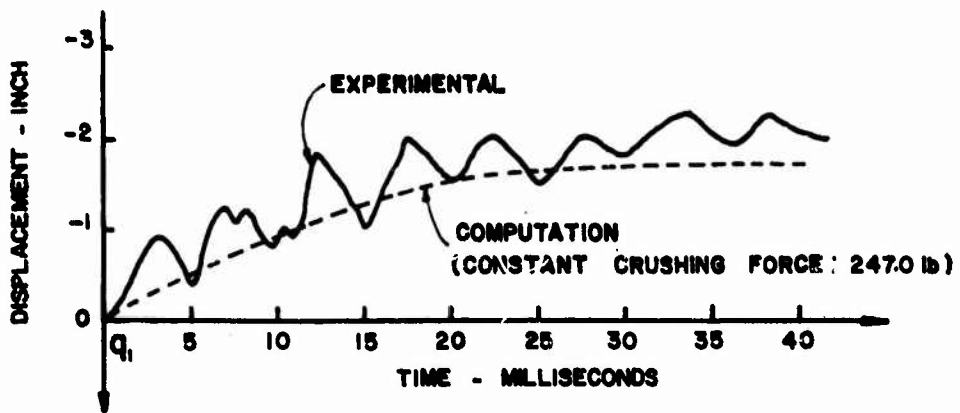


(b) COORDINATE q_{10}

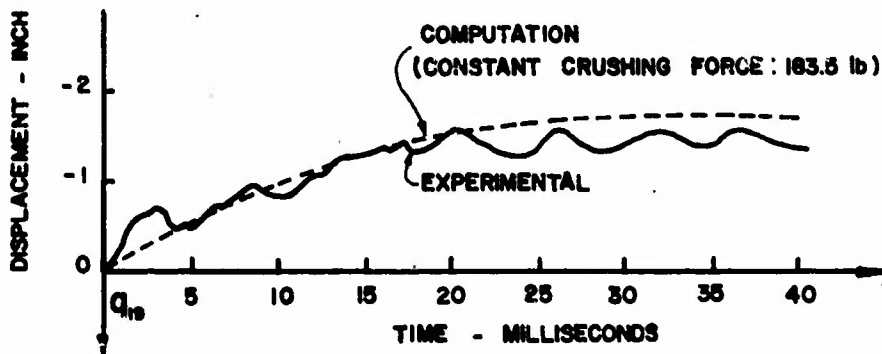


(c) COORDINATE q_5

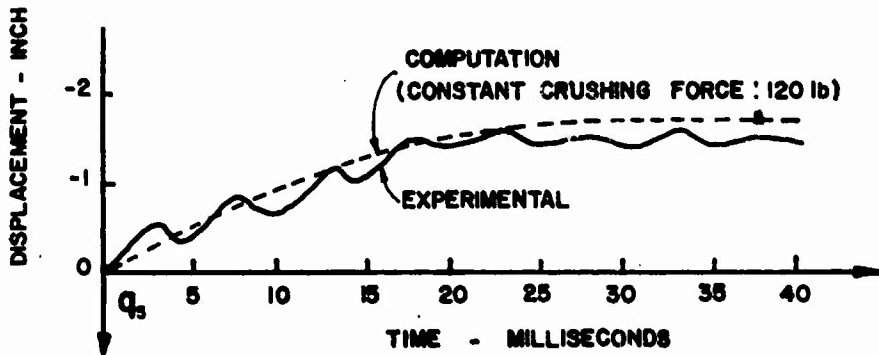
FIG. 13 MEASURED AND COMPUTED VALUES OF q_1 , q_5 AND q_{10} WITHOUT THE 3% (2.3 lb.) UNCUSHIONED MASS AT q_{11} (DROP HEIGHT 18 INCHES)



(a) COORDINATE q_1

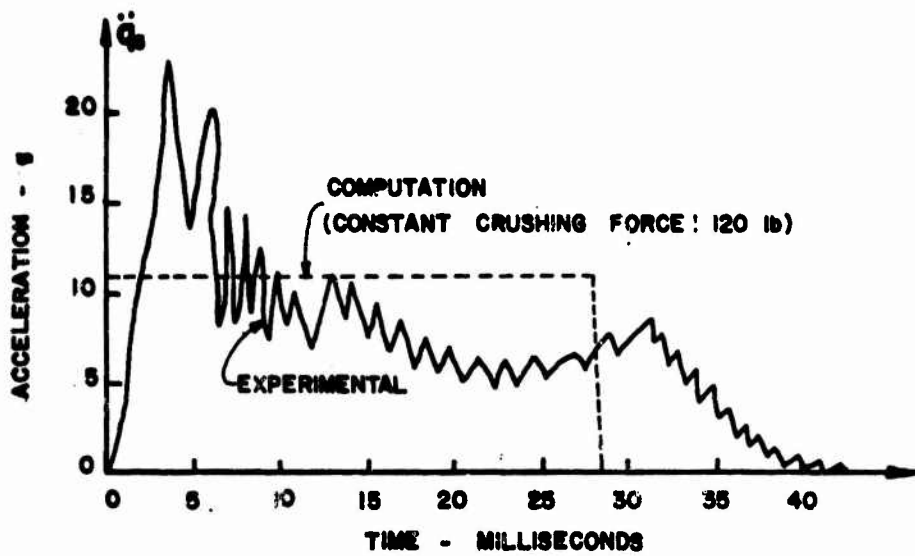


(b) COORDINATE q_{19}

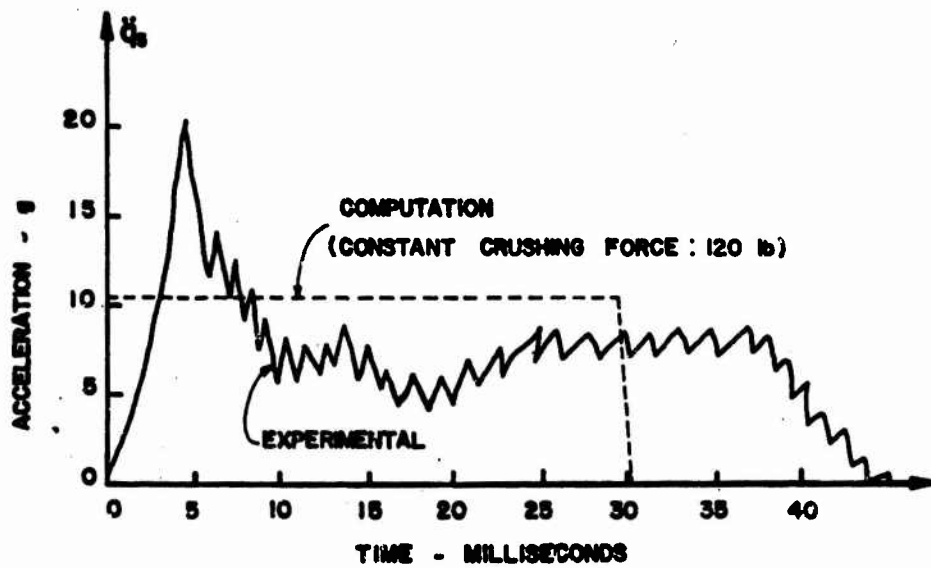


(c) COORDINATE q_5

FIG.14 MEASURED AND COMPUTED VALUES OF q_1 , q_5 AND q_{19} WITH 3% (2.3 lb.) UNCUSHIONED MASS AT q_{11} (DROP HEIGHT 18 INCHES)

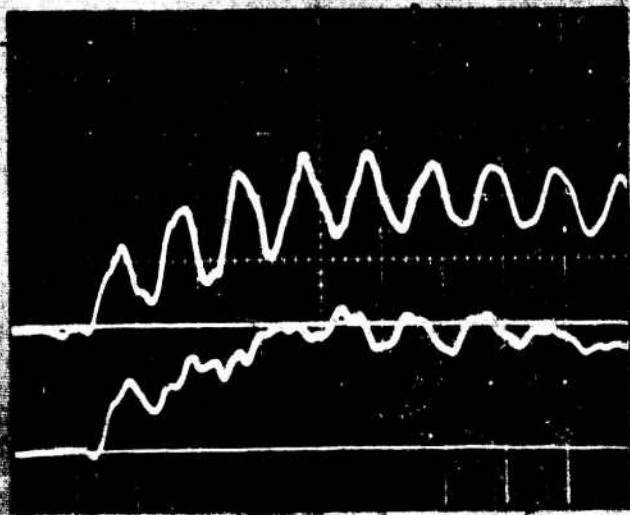


(a) WITHOUT 3% UNCUSHIONED MASS AT q_{11}



(a) 3% UNCUSHIONED MASS AT q_{11}

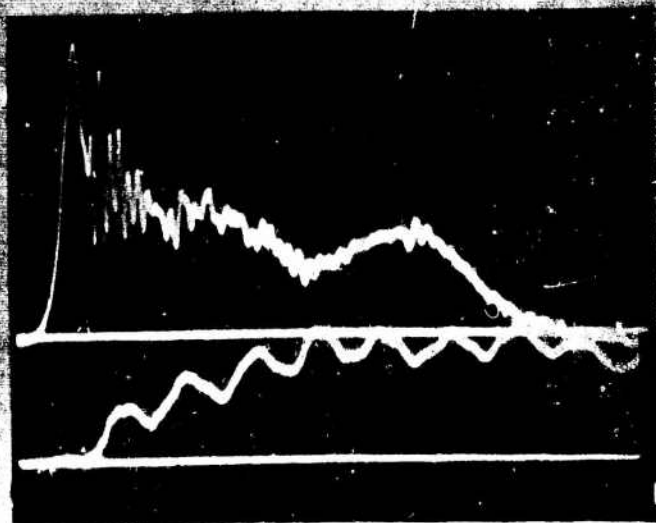
FIG. 15 MEASURED AND COMPUTED VALUES OF ACCELERATION OF q_5 (DROP HEIGHT 18 INCHES)



q_1 - DISPLACEMENT
 0.5"/DIV
 q_2 - DISPLACEMENT
 0.25"/DIV

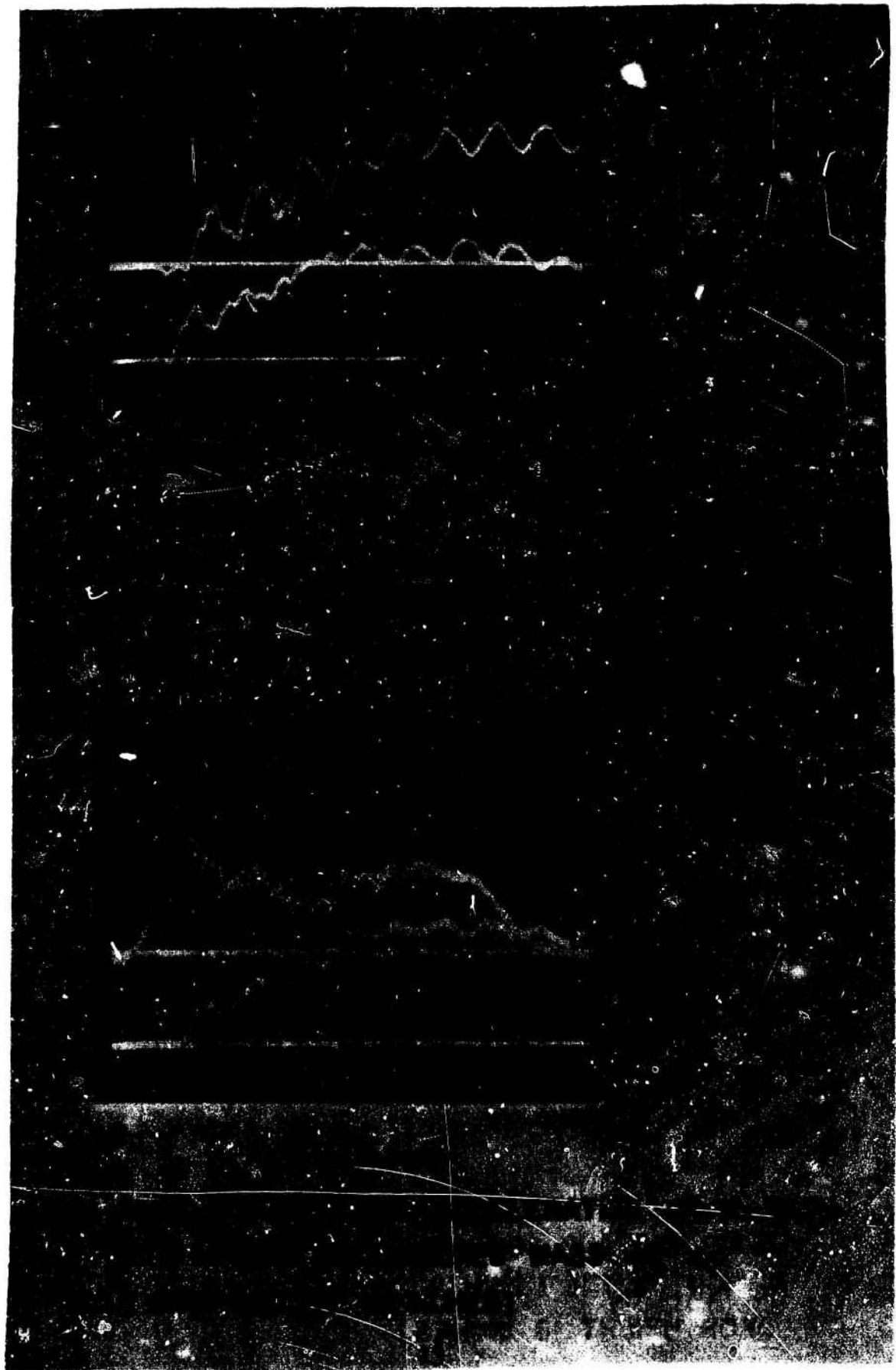
T
 5 MILLISECONDS / DIV

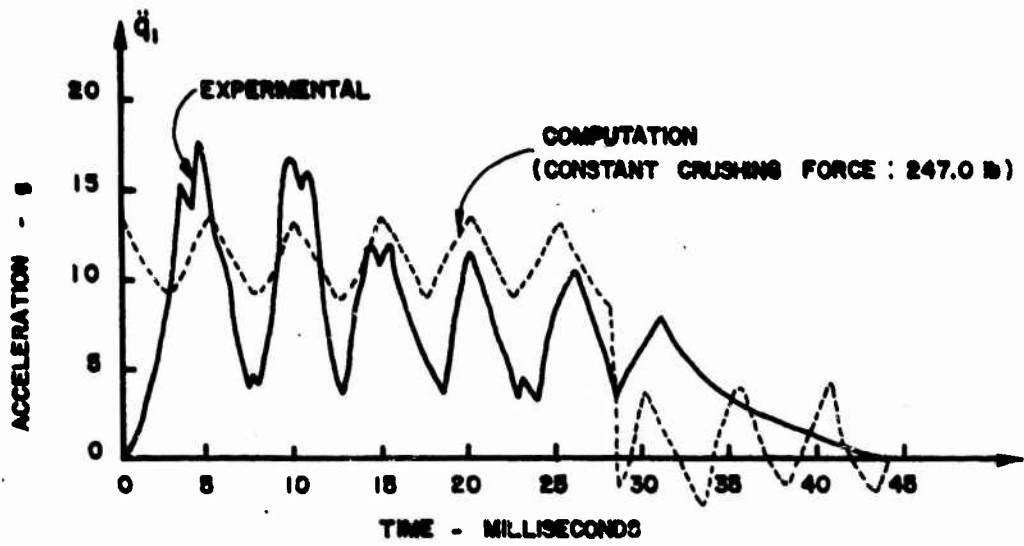
DISPLACEMENTS q_1 AND q_2 WITHOUT 2.3 lb (3%)
 UNCUSHIONED MASS AT q_1
 (DROP HEIGHT 18 INCHES)



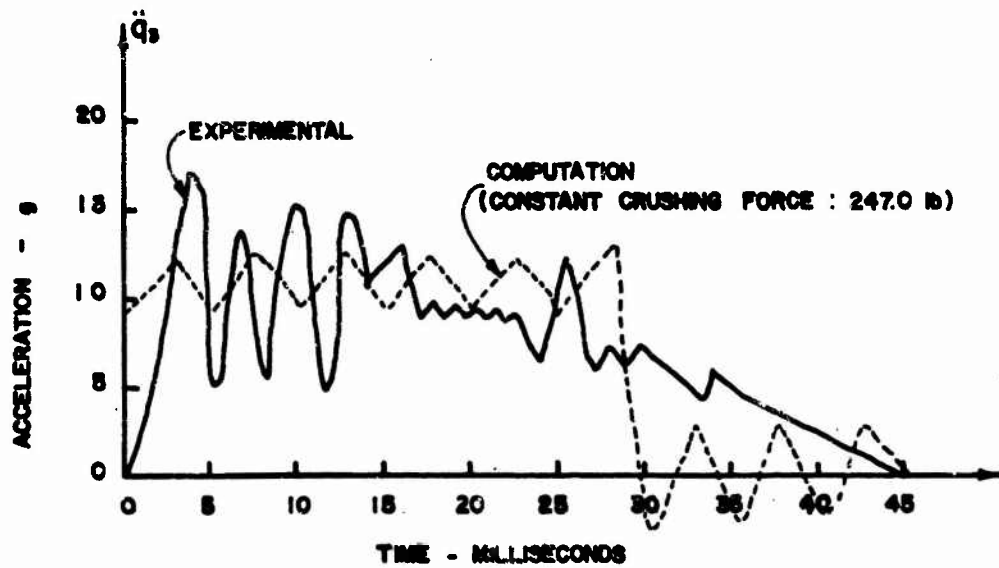
T
 5 MILLISECONDS / DIV

FIG.17 DISPLACEMENT AND ACCELERATION OF M_1 WITH-
 -OUT 2.3 lb (3%) UNCUSHIONED MASS AT q_1
 (DROP HEIGHT 18 INCHES)





(a) COORDINATE q_1



(b) COORDINATE q_3

FIG. 20 MEASURED AND COMPUTED VALUES OF q_1 AND q_3 WITHOUT 2.3 lb (3%) UNCUSHIONED MASS AT q_{11} (DROP HEIGHT 18 INCHES)

Figs. 15 and 20. The computed accelerations for M_2 , shown in Fig. 15, are almost identical in form to the assumed cushioning force, while the measured accelerations closely resemble the general form of the crushing force-time-relation for paper honeycomb usually observed. The rather high frequency oscillations which appear on the measured acceleration record are also somewhat typical of the oscillations seen on dynamic stress-strain curves for paper honeycomb. The source of these oscillations can not always be pinpointed. In some cases they are believed to typify the way honeycomb actually crushes, in others they are believed to represent vibration of some part of the testing system. In these records the frequency is much too high to be the uncoupled frequency of M_2 and its supporting spring, and too low to be associated with the elastic body vibration of the mass. Consequently the oscillations are attributed to the crushing characteristics of the honeycomb cushions.

The oscillations which appear in the displacement, and both the measured and computed accelerations of M_1 all have very nearly the same frequency, approximately 200 Hertz. This is also the uncoupled frequency of M_1 . It is somewhat surprising to see oscillations of a mass as large as M_1 at 200 Hertz. If the peak accelerations associated with the oscillations of the mass are computed assuming a steady state harmonic oscillation they are found to be of the order of 2000g whereas the computed accelerations do not exceed peak values of about 2g, and the measured values are of the order of 6g. Thus the oscillations on the displacement record are not believed to be connected with actual motion of the mass. They are believed to be a result of vibration of the displacement gage. The fact that they occur at nearly the same frequency as the oscillations in the acceleration records is probably just coincidence. If the oscillations are ignored, and the actual curve replaced by a smoothed curve in each of the 6 records shown in Figs. 13 and 14 the measured and computed displacements are seen to be in quite good agreement considering the differences in the crushing forces discussed above. Differences between the measured and computed deflections would undoubtedly be much greater if it were not for the relative insensitivity of displacement to the form of the acceleration curve.

The oscillations which appear in the computed acceleration record for $M_2(\ddot{u}_3)$ shown in Fig. 20 have a frequency which is nearly equal to the uncoupled frequency of M_2 . No mass in the system will vibrate at its uncoupled frequency since

there is coupling between all masses in the system. Consequently the observed frequency should not be expected to agree with the uncoupled frequency. The frequency of the oscillations in the measured acceleration is almost twice the frequency seen in the computed accelerations. No logical explanation for this discrepancy can be offered at this time.

Although the computed and measured values of the displacements and accelerations do not agree precisely they are close enough, it is believed, to indicate that with the same crushing force in the two models the results could be brought into close agreement. This means that the continuous laboratory system can be replaced for computations by a lumped parameter system which will adequately represent the essential features of the motion of the major parts of the laboratory model. Hence, a vehicle could be represented in the same way.

It may be further noted that the addition of the small mass M_7 does not significantly affect the displacements and accelerations of the other masses. This means that only the major masses in a physical system need to be represented in the lumped parameter model.

8. Conclusions

Although the comparisons between computed and experimental results are not exhaustive, and there is a significant difference in crushing forces in the two models, the following conclusions are believed to be justified.

- a. Displacements, velocities, and accelerations of the principal parts of a laboratory model can be satisfactorily predicted using a lumped parameter mathematical model and a numerical computation procedure.
- b. If predictions can be made for a laboratory model, then predictions of comparable accuracy are possible for actual prototype vehicles.
- c. The computed program is simple enough, and the computational time required is short enough to make the program a practical tool for design purposes.
- d. The insignificant effect which the small masses have on the motions of the larger masses in the system indicates that models of prototype vehicles can be quite simple and still give an accurate indication of the movements of the different parts during an impact.

e. Procedures for establishing parameter values such as mass, and stiffness, for lumped parameter models to represent actual vehicles are not indicated in the results of this study. These procedures remain to be developed.

9. Recommendations for Further Studies

a. Although the results obtained for the one dimensional model were not entirely conclusive, further work should be concentrated on a two dimensional lumped mass model. For the theoretical analysis of such a model it is necessary only to modify the stiffness matrix as a grid structure. A grid structure would not only be a more realistic representation of a real vehicle body, it would also make the laboratory model more stable. This would improve the accuracy of measurements.

b. The damping factor which was not considered in this report should be investigated in further studies. This can be done rather easily mathematically but the question of how to introduce controlled damping into the laboratory model requires some study.

c. An actual vehicle for which measurement data are available, or can be obtained, should be modeled so the procedure can be tested in a real life situation.

d. The significance of the parameters which are being determined should be carefully reviewed in the context of vehicle damage.

References

1. Ellis, B. C., E. A. Ripperger and J. Neils Thompson, Design of Cushioning System for Air Delivery of Equipment, Structural Mechanics Research Laboratory, The University of Texas (Austin) 1958.
2. Hurty, W. C. and M. F. Rubinstein, Dynamics of Structures, Chapter 2, Englewood Cliffs, N.J., Prentice-Hall, 1964.
3. Schied, Francis, Theory and Problems of Numerical Analysis, Chapter 20, New York, McGraw-Hill Book Co., 1968.

APPENDIX

Flow Chart and Computer Program

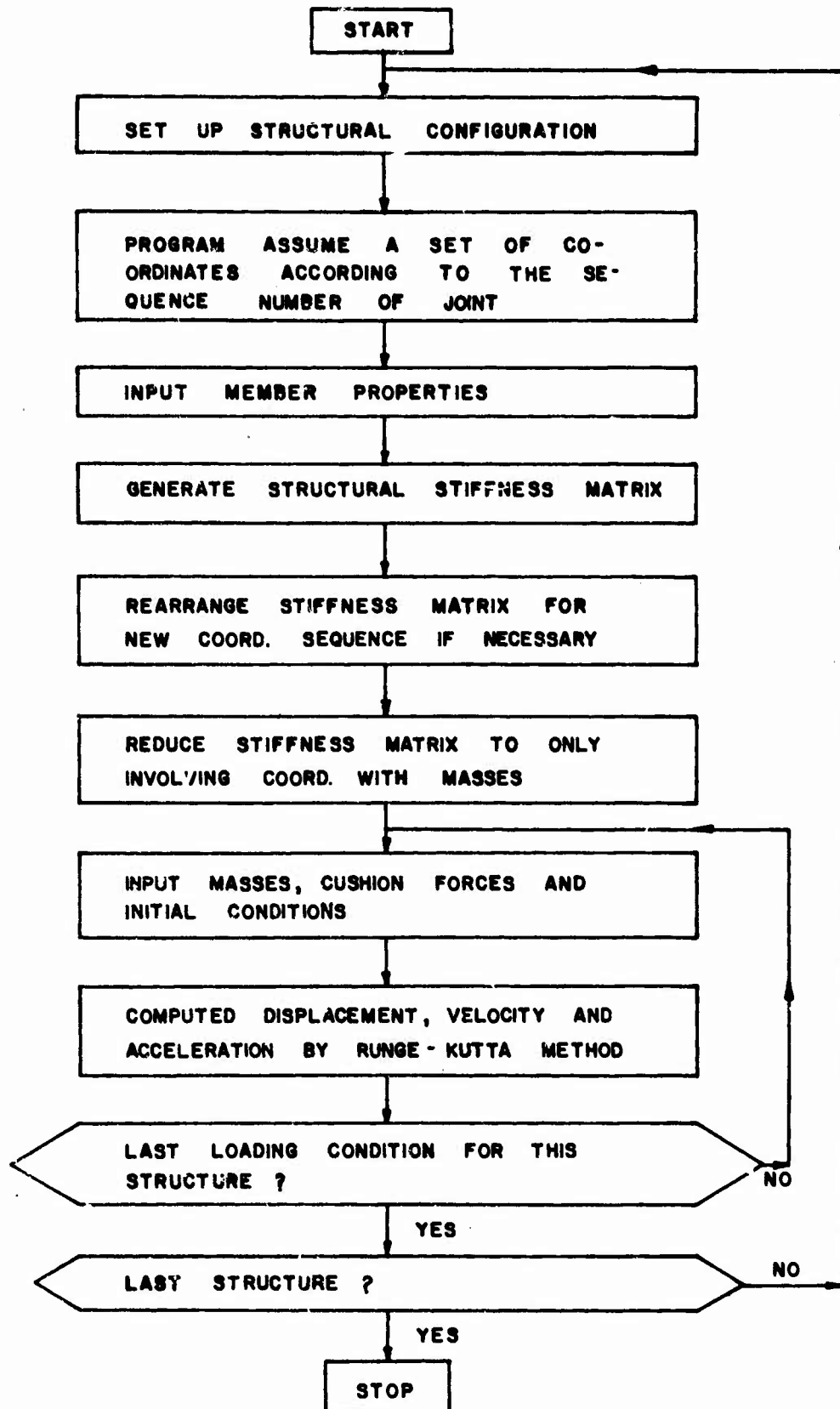


FIG.21 MAIN PROGRAM FLOW CHART

```

C     NUMERICAL SOLUTION OF A LUMPED PARAMETER FOR AIRDROPPED
C     VEHICLES BY USING RUNGE-KUTTA METHOD.
C     CDC 6600 ,  FORTRAN IV ,  STORAGE REQUIRED  30000 WORDS
C     DIMENSION  SK(30,30) ,NOD(30),U(30,30),C(30,30),NV(30), SQ(30)
C     DIMENSION  DF(10,100),YJ(100) ,YJO(100)
C     DIMENSION  YJ3(30),  SQ3(30)
C     COMMON  N,S(30,30),GQA(30),WM(30),WG(30)
5010  FORMAT(3I10,F20.2)
5020  FORMAT(2I10,2F20.4)
5040  FORMAT(16I5)
5050  FORMAT(8F10.3)
5060  FORMAT(16F5.1)
6010  FORMAT(1H1,* BEAM MBR=*,I5,2X,*SPRING NO.=* I5,2X,*TOTAL JNT NO.=*
1     ,I5,2X,*E=*,F12.2)
6020  FORMAT(14,12F11.0/(4X,12F11.0))
C --  INITIALLY THE PROGRAM ASSIGNS  A SET OF COORD. ACCORDING TO THE
C     ORDER OF JOINT NUMBER .  IT BECOMES, FOR EXAMPLE, Q(11) AND Q(12)
C     OR THE VERTICAL DISPLACEMENT  AND THE ROTATION AT JOINT NUMBER 6.
C --- READ IN  NS =NO. OF STRUCTURES
C             N11=NO. OF COORD. WITH ASSOCIATED MASSES
C             N22=NO. OF COORD. WITHOUT ASSOCIATED MASSES
C             NCH= 1 ,  IF THE ORDER OF COORD. WILL BE REARRANGED
C             NCH= 0 ,  NO REARRANGEMENT IN COORDINATE ORDER.
      READ( 5,5040)  NS
1     READ(5,5040)  N11,N22,NCH
      JC=N11+N22
C --- READ IN  MBR= NO. OF BEAM MEMBERS
C             NP = NO. OF SPRINGS
C             JNT= TOTAL JOINT NUMBER
C             E  = MODULUS OF ELASTICITY
      READ(5,5010)  MBR,NP,JNT,E
      WRITE (6,6010)  MBR,NP,JNT,E
      G=386.04
      N=2*N11
      MT=MBR+NP
      JM=JNT-NP
      JC=2*JNT-NP      $ JNT1=JC-1
      DO 5 I=1,JC
      DO 5 J=1,JC
5     SK(I,J)=0.
      DO 100 I=1,MT
C --- READ IN MEMBER PROPERTIES,
C     JOINT NUMBERS CAN BE ASSIGNED ARBITRARILY IN THE ORDER BUT
C     SHOULD BE CONTINUOUS FROM 1 THROUGH THE LAST JOINT NUMBER,
C     NO NUMBER IN THIS INTERVAL CAN BE OMITTED.  ALL SPRING JOINTS
C     NOT ATTACHED TO BEAMS SHOULD ALSO BE NUMBERED FOLLOWING THE
C     BEAM JOINT NUMBERS.
C     NJ1, NJ2= JOINT NUMBERS  AT ELEMENT ENDS
C     AI= MOMENT OF INERTIA  FOR BEAM MEMBER, OR SPRING CONSTANT
C     SL= LENGTH OF BEAM SEGMENT ,
C     SL= 0.0  FOR SPRING
      READ(5,5020)  NJ1,NJ2,AI,SL
      WRITE (6,5020)  NJ1,NJ2,AI,SL
      IF(SL) 20,20,10
C --- GENERATE STIFFNESS MATRIX OF STRUCTURE

```

```

10  FA=E*AI/SL**3
    S1=12.*FA $ S2=6.*SL*FA $ S3=2.*SL*SL*FA $ S4=2.*S3
    IF(NJ1-NJ2) 11,11,12
11  N1=2*NJ1-1 $ N3=2*NJ2-1
    GO TO 16
12  N1=2*NJ2-1 $ N3=2*NJ1-1
16  N2=N1+1 $ N4=N3+1
    SK(N1,N1)=SK(N1,N1)+S1 $ SK(N1,N2)=SK(N1,N2)-S2
    SK(N1,N3)=SK(N1,N3)-S1
    SK(N1,N4)=SK(N1,N4)-S2 $ SK(N2,N2)=SK(N2,N2)+S4
    SK(N2,N3)=SK(N2,N3)+S2
    SK(N2,N4)=SK(N2,N4)+S3
    SK(N3,N3)=SK(N3,N3)+S1 $ SK(N3,N4)=SK(N3,N4)+S2
    SK(N4,N4)=SK(N4,N4)+S4
    GO TO 100
20  IF(NJ1-JM) 30,30,32
30  N1=NJ1*2-1
    GO TO 40
32  N1=NJ1+JM
40  IF(NJ2-JM) 50,50,55
50  N2=NJ2*2-1
    GO TO 60
55  N2=NJ2+JM
60  CONTINUE
    SK(N1,N1)=SK(N1,N1)+AI $ SK(N2,N1)=SK(N2,N1)-AI
    SK(N2,N2)=SK(N2,N2)+AI
100 CONTINUE
    N1=JC-1
    IF(NCH) 280,280,210
C --- READ IN NOD(I)=NEW ORDER OF COORD.
C --- ALL INPUT AND OUTPUT FROM HERE ON ARE REFERRED TO THIS
C --- NEW COORDINATES SYSTEM
210 READ(5,5040) (NOD(I),I=1,JC)
    WRITE(6,5040) (NOD(I),I=1,JC)
    I=JC
220 J=NOD(I)
    SK(I,1)=SK(J,J)
    I=I-1
    IF(I) 230,230,220
230 DO 240 I=1,JC
240 SK(I,I)=SK(I,1)
    DO 260 J=1,N1
    J1=J+1
    JP=NOD(J)
    DO 260 I=J1,JC
    IP=NOD(I)
    IF(IP-JP) 251,251,252
251 SK(I,J)=SK(IP,JP)
    GO TO 260
252 SK(I,J)=SK(JP,IP)
260 CONTINUE
280 CONTINUE
    DO 270 J=1,N1
    I1=J+1
    DO 270 I=I1,JC

```

```

SK(J,I)=SK(I,J)
270 CONTINUE
DO 140 I=1,JC
140 WRITE(6,6020) I,(SK(I,J),J=1,JC)
CALL MIV(SK,U,N11,N22)
DO 320 I=1,N11
DO 320 J=1,N22
SUM=0.
DO 310 K=1,N22
K1=K+N11
310 SUM=SUM+SK(I,K1)*U(K,J)
C(I,J)=SUM
320 CONTINUE
DO 340 I=1,N11
DO 340 J=1,N11
SUM=0.
DO 330 K=1,N22
K1=K+N11
330 SUM=SUM+C(I,K)*SK(K1,J)
340 S(I,J)=SK(I,J)-SUM
DO 341 I=1,N11
341 WRITE (6,6020) I,(S(I,J),J=1,N11)
339 CONTINUE
C --- READ IN H = TIME STEP SIZE OF INTEGRATION IN RUNGE-KUTTA METHOD.
C H = 0.0 OR BLANK FOR STARTING NEXT STRUCTURE OR
C LAST CARD OF INPUT DATA DECK
C DT= TIME INTERVAL OF PRINT OUT
C TEND=END OF TIME OF CALCULATION
READ(5,5050) H,DT,TEND
IF(H.EQ. 0.) GO TO 380
READ (5,5040) LM,LW,LT,LV,LS
NGO=0
IF(LM) 343,343,342
342 NGO=NGO+1
READ(5,5050) (WM(I),I=1,N11)
C--- READ IN WM(I)= MASSES (IF LM GREATER THAN 0)
C WG(I)=STATIC REACTION AT CUSHIONED COORD. (IF LW .GT. 0)
C NT=TOTAL NUMBER OF CUSHIONED COORD. (IF LT .GT. 0)
C NV(I)=CUSHIONED COORD.
C VO=EQUIVALENT FREE FALL VELOCITY (IF LV .GT. 0)
C YJO(I)=1. AT ALL VERTICAL DISPLACEMENTS
C YJO(I)=0. AT ROTATIONAL COORD.
C SQ(I)=CUSHIONING FORCES (IF LS .GT. 0)
343 WRITE(6,5050) (WM(I),I=1,N11)
IF(LW) 345,345,344
344 NGO=NGO+1
READ( 5,5050) (WG(I),I=1,JC)
345 WRITE(6,5050) (WG(I),I=1,JC)
IF(LT) 347,347,346
346 NGO=NGO+1
READ(5,5040) (NT, (NV(I),I=1,NT))
347 WRITE(6,5040) (NT, (NV(I),I=1,NT))
IF(LV) 349,349,348
348 NGO=NGO+1
READ(5,5050) VO

```

```

WRITE(6,5050)  V0
READ( 5,5060)  (YJ0(I),I=1,JC)
DO 351  I=1,JC
YJ0(I)=V0*YJ0(I)
351  YJ3(I)=YJ0(I)
GO TO 353
349  DO 352  I=1,JC
352  YJ0(I)=YJ3(I)
353  WRITE(6,5050)  (YJ0(I),I=1,JC)
IF(LS) 355,355,354
354  NGO=NGO+1
350  READ( 5,5050)  (SQ(I),I=1,JC)
DO 359  I=1,JC
359  SQ3(I)=SQ(I)
GO TO 357
355  DO 356  I=1,JC
356  SQ(I)=SQ3(I)
357  WRITE(6,5050)  (SQ(I),I=1,JC)
IF(NGO) 380,380,358
358  CONTINUE
DO 21  I=1,JC
J=I*2
YJ(J-1)=0.
21  YJ(J)=YJ0(I)
DO 370  I=1,N11
SUM=0.
DO 360  J=1,N22
J1=J+N11
360  SUM=SUM+C(I,J)*SQ(J1)
GQA(I)=SQ(I)-SUM
370  CONTINUE
WRITE(6,5050)  (GQA(I),I=1,N11)
PRINT 385
385  FORMAT( 1H1, //,4X,*COORD*,10X,*DISP.*,15X,*VELOCITY*,12X,*ACC.*)
CALL RKAMSB(3,1.0E-7,1.0,1.0E-10,1.0E-8,0.0)
ALPHA=0.0
K5=2*JC
DO 141  I=1,K5
141  YJ0(I)=YJ(I)
390  OMEGA=ALPHA+DT
IF(OMEGA.GT.TEND) GO TO 339
150  CALL RKAMSB(1,ALPHA,OMEGA,H,SSE,YJ)
PRINT 14,OMEGA
14  FORMAT(20X,3H T=, F15.6)
CALL DERFCN ( OMEGA,YJ,1,DF)
DO 15  I=2,N,2
I1=I/2
I2=I-1
15  WRITE(6,6001)  I1,YJ(I2),YJ(I),DF(1,I)
NI=N11+1
DO 410  I=NI,N
SUM=0.
DO 400  J=1,N11
J1=J*2-1
400  SUM=SUM+SK(I,J)*YJ(J1)

```

```

GQA(I)=SQ(I)-SUM
410 CONTINUE
DO 430 I=1,N22
SUM=0.
DO 420 J=1,N22
J1=J+N11
420 SUM=SUM+U(I,J)*GQA(J1)
I1=N11+I
K1=I1*2-1
K2=K1+1
YJ(K1)=SUM
YJ(K2)=(SUM-YJ0(K1))/DT
DF(1,I1)=(YJ(K2)-YJ0(K2))/DT
WRITE(6,6001) I1,SUM ,YJ(K2),DF(1,I1)
430 CONTINUE
MQ=0
DO 515 I=1,NT
J=NV(I)
K=J*2
460 IF(YJ0(K)*YJ(K)) 470,515,515
470 IF(SQ(J)) 480,490,490
480 SQ(J)=0.0
GO TO 500
490 SQ(J)=-WG(J)
500 MQ=1
515 CONTINUE
IF(MQ ) 550,550,520
520 DO 540 I=1,N11
SUM=0.
DO 530 J=1,N22
J1=J+N11
SUM=SUM+C(I,J)*SQ(J)
530 CONTINUE
540 GQA(I)=SQ(I)-SUM
550 CONTINUE
ALPHA=OMEGA
GO TO 390
380 CONTINUE
NS=NS-1
IF(NS) 26,26,1
6001 FORMAT(5X,I4,4E20.5)
26 STOP
END

```

```

SUBROUTINE RKAMSB(MODE,A1,A2,A3,A4,YJ)
DIMENSION X(10),Y(10,100),YJ(100),D(10,100),DF(10,100),XS(10),
1 W(10),B(10,100),A(10),BP(10),BC(10),PHI(100),YS(10,100)
DOUBLE Y,PHI,YS
COMMON N,S(30,30),GQA(30),WM(30),WG(30)
GO TO (2,2,1),MODE
1 CONTINUE
C ----- COEFFICIENTS
W(1)=W(4)=1./6. $ W(2)=W(3)=1./3. $ KK=4
A(2)=A(3)=.5 $ A(4)=1.
B(2,1)=B(3,2)=.5 $ B(3,1)=B(4,1)=B(4,2)=0. $ B(4,3)=1.
IQ = 4 $ FCT = 19./270.
BP(1)=-9./24. $ BP(2)=37./24. $ BP(3)=-59./24. $ BP(4)=55./24.
BC(1)=1./24. $ BC(2)=-5./24. $ BC(3)=19./24. $ BC(4)=9./24.
C ----- TOLERANCES
HMIN=A1 $ HMAX=A2 $ EMIN=A3 $ EMAX=A4 $ ISKIP = 1
IF( YJ(1).EQ.0.) ISKIP = 0
RETURN
2 CONTINUE
C ----- RKAMSUB ENTRY POINT
CALL DERFCN(A1,YJ,1,DF)
ALPHA = A1 $ OMEGA = A2 $ H = A3
IF( MODE.EQ.2 ) IQ = KK
IQM1 = IQ-1 $ IQP1 = IQ+1 $ ISTEP=0 $ SIGN=1.
IF( H.LT.0. ) SIGN = -1.
X(1) = ALPHA
DO 3 I=1,N
3 Y(1,I) = YJ(I)
4 MM = 1 $ IFLG = 0
5 KCOUNT = 0
6 M = MM $ MM = M + 1
IF( MM.GT.IQP1 ) MM = 1
X(MM) = X(M) + H
TEST = OMEGA - X(MM) $ TEST1=TEST/OMEGA
IF QUOTIENT OVERFLOW 7,8
7 TEST1 = TEST
8 IF( ABS(TEST1).LT.1.0E-10 ) GO TO 12
IF( SIGN*TEST1 ) 9,12,13
9 TEST2 = OMEGA - X(M)
IF( MODE.EQ.2 ) GO TO 11
IF( ISKIP.EQ.0.OR.SIGN*TEST2.LT.HMIN ) GO TO 99
H = TEST2/IQ
IF( SIGN*H.LT.HMIN ) GO TO 11
M = M-1
IF( M.EQ.0 ) M=IQP1
X(1) = X(M)
DO 10 I=1,N
10 Y(1,I) = Y(M,I)
GO TO 4
11 H = TEST2 $ IFLG = 0
X(MM) = X(M) + H
12 ISTEP = 1
13 XJ = X(M)
DO 14 I=1,N
14 YJ(I) = Y(M,i)

```



```

      IF( MODE.EQ.1.AND.M.EQ.IQ.OR.IFLG.EQ.1 ) GO TO 32
C ----- RUNGE-KUTTA PROCEDURE
      DO 25 K=1,KK
      IF( K.EQ.1 ) GO TO 22
      XJ = X(M) + H*A(K)
      DO 15 I=1,N
15  PHI(I) = 0.
      KMJ = K - 1
      DO 20 I=1,N
      DO 19 J=1,KMJ
19  PHI(I) = PHI(I) + H*B(K,J)*D(J,I)
20  YJ(I) = Y(M,I) + PHI(I)
22  CALL DERFCN(XJ,YJ,K,D)
      IF( IFLG.EQ.2.OR.K.NE.1 ) GO TO 25
      DO 23 I=1,N
23  DF(M,I) = D(1,I)
25  CONTINUE
      DO 27 I=1,N
27  PHI(I) = 0.
      DO 30 I=1,N
      DO 29 K=1,KK
29  PHI(I) = PHI(I) + H*W(K)*D(K,I)
30  Y(MM,I) = Y(M,I) + PHI(I)
      IF( ISTEP.EQ.1 ) GO TO 100
      GO TO 6
C ----- ADAMS PREDICTOR-CORRECTOR PROCEDURE
32  CALL DERFCN(XJ,YJ,M,DF)
      DO 33 I=1,N
33  PHI(I) = 0.
      DO 34 K=1,IQ
      J = K + KCOUNT
      IF( J.GT.IQP1 ) J = J - IQP1
      DO 34 I=1,N
34  PHI(I) = PHI(I) + H*BP(K)*DF(J,I)
      DO 35 I=1,N
35  YJ(I) = Y(M,I) + PHI(I)
      XJ = X(MM)
      CALL DERFCN(XJ,YJ,MM,DF)
      DO 43 I=1,N
43  PHI(I) = 0.
      DO 44 K=1,IQ
      J = K + KCOUNT + 1
      IF( J.GT.IQP1 ) J = J - IQP1
      DO 44 I=1,N
44  PHI(I) = PHI(I) + H*BC(K)*DF(J,I)
      DO 45 I=1,N
45  Y(MM,I) = Y(M,I) + PHI(I)
C ----- SINGLE-STEP ERROR
      DLTMX = 0.
      DO 54 I=1,N
      DLT = ABS( Y(MM,I) - YJ(I) )
      IF( DLT.LE.DLTMX ) GO TO 54
      DLTMX = DLT $ IDLT = I
54  CONTINUE
      TEST = DLTMX/Y(MM,IDLT)

```

```

      IF QUOTIENT OVERFLOW 55,56
55 SSE = ABS( FCT*DLTMX ) $ GO TO 60
56 SSE = ABS( FCT*TEST )
60 CONTINUE
C ----- ERROR ANALYSIS
      IF( ISKIP.EQ.0 ) GO TO 90
      IF( EMIN.LT.SSE.AND.SSE.LT.EMAX ) GO TO 90
      IF( SIGN*H.GT.HMIN.AND.SIGN*H.LT.HMAX ) 65,89
65 IF( SSE.GT.EMAX ) 66,70
66 H = H/2.
      IF( SIGN*H.LT.HMIN ) 89,68
68 IF( IFLG.EQ.0 ) GO TO 4
      M = M-1
      IF( M.EQ.0 ) M = IQP1
      X(1) = X(M)
      DO 69 I=1,N
69 Y(1,I) = Y(M,I)
      GO TO 4
70 IF( ISTEP.EQ.1 ) GO TO 100
73 H = 2.*H
      IF( SIGN*( X(MM)+H-OMEGA ) ) 77,75,75
75 H = H/2. $ GO TO 90
77 IF( SIGN*H.GT.HMAX ) 89,78
78 IBK = IQ/2 + 1 $ L = 0
      DO 82 K=1,IBK
      J = IBK - K + 1 $ M = MM - L
      IF( M.LE.0 ) 79,80
79 M = M + IQP1 $ L = 0 $ MM = M
80 XS(J) = X(M)
      DO 81 I=1,N
      D(J,I) = DF(M,I)
81 YS(J,I) = Y(M,I)
82 L = L + 2
      DO 85 K=1,IBK
      X(K) = XS(K)
      DO 85 I=1,N
      DF(K,I) = D(K,I)
85 Y(K,I) = YS(K,I)
      MM = IBK $ IFLG = 2 $ GO TO 5
89 PRINT 511 $ GO TO 100
90 IF( ISTEP.EQ.1 ) GO TO 100
      IFLG = 1 $ KCOUNT=KCOUNT+1
      IF( KCOUNT.EQ.IQP1 ) KCOUNT = 0
      GO TO 6
99 MM = M
100 CONTINUE
C ----- RKAMSUB EXIT POINT
      A2 = X(MM) $ A3 = H $ A4 = SSE
      DO 105 I=1,N
105 YJ(I) = Y(MM,I)
511 FORMAT(1H1,5X,25H STEP SIZE OUT OF BOUNDS )
500 RETURN $ END

```

```

SUBROUTINE DERFCN (XJ,YJ,M,DF)
COMMON N,S(30,30),GQA(30),WM(30),WG(30)
DIMENSION DF(10,100),YJ(100)
N1=N/2
DO 10 I=1,N,2
10 DF(M,I)=YJ(I+1)
DO 30 I=2,N,2
SUM=0. $ I1=I/2
DO 20 J=1,N1
J1=J*2-1
J2=J1+1
20 SUM=SUM+S(I1,J)*YJ(J1)
30 DF(M,I)=(GQA(I1)-SUM)/WM(I1)
RETURN $ END

```

```

SUBROUTINE MIV(SK,U,N1,NM)
DIMENSION A(30,30),U(30,30),SK(30,30)
DO 9001 I=1,NM
I1=I+N1
DO 9001 J=1,NM
J1=J+N1
A(I,J)=SK(I1,J1)
U(I,J)=0.
IF (I.EQ.J) U(I,J)=1.0
9001 CONTINUE
EPS=0.0000001
DO 9015 I=1,NM
K=I
IF (I-NM) 9021,9007,9021
9021 IF (A(I,I)-EPS) 9005,9006,9007
9005 IF (-A(I,I)-EPS) 9006,9006,9007
9006 K=K+1
DO 9023 J=1,NM
U(I,J)=U(I,J)+U(K,J)
9023 A(I,J)=A(I,J)+A(K,J)
GO TO 9021
9007 DIV=A(I,I)
DO 9009 J=1,NM
U(I,J)=U(I,J)/DIV
9009 A(I,J)=A(I,J)/DIV
DO 9015 MM=1,NM
DELT=A(MM,I)
IF (ABS(DELT)-EPS) 9015,9015,9016
9016 IF (MM-I) 9010,9015,9010
9010 DO 9011 J=1,NM
U(MM,J)=U(MM,J)-U(I,J)*DELT
9011 A(MM,J)=A(MM,J)-A(I,J)*DELT
9015 CONTINUE
RETURN $ END

```

UNCLASSIFIED
Security Classification

DOCUMENT CONTROL DATA - R & D

(Security classification of title, body of abstract and indexing annotation must be entered when the overall report is classified)

1. ORIGINATING ACTIVITY (Corporate author) University of Texas at Austin Austin, Texas		2a. REPORT SECURITY CLASSIFICATION UNCLASSIFIED	
		2b. GROUP	
3. REPORT TITLE The Effect of Airdrop Impact on Complex Structures			
4. DESCRIPTIVE NOTES (Type of report and inclusive dates) Final Report			
5. AUTHOR(S) (First name, middle initial, last name) Song Fong Jan E. A. Ripperger			
6. REPORT DATE December 1969		7a. TOTAL NO. OF PAGES 39	7b. NO. OF REFS 3
8a. CONTRACT OR GRANT NO. DAAG 17-67-C-0189		8b. ORIGINATOR'S REPORT NUMBER(S)	
a. PROJECT NO. 1M121401D195			
c.		9b. OTHER REPORT NO(S) (Any other numbers that may be assigned this report) 70-55-AD	
d.			
10. DISTRIBUTION STATEMENT This document has been approved for public release and sale; its distribution is unlimited.			
11. SUPPLEMENTARY NOTES		12. SPONSORING MILITARY ACTIVITY US Army Natick Laboratories Natick, Massachusetts 01760	
13. ABSTRACT The accelerations and displacements in a complex structure subjected to an impact loading are computed by treating the structure as a lumped parameter system. A mathematical model of the system consists basically of discrete masses linked by weightless, elastic beams with the appropriate stiffnesses, areas, and moment of inertia properties. By specifying a proper set of independent coordinates through which the motion of these lumped masses are uniquely described, and by writing equations of motion in terms of these coordinates, a set of equations is derived which represents the motion of any part of the model during impact. Using the Runge-Kutta numerical method, and a digital computer, these equations are solved. A physical model of the lumped parameter system was built and cushioned with paper honeycomb. Displacements and accelerations at some points in this model were measured and compared with computed results. Agreement is satisfactory.			

DD FORM 1473
NOV 66

REPLACES DD FORM 1473, 1 JAN 64, WHICH IS OBSOLETE FOR ARMY USE.

UNCLASSIFIED
Security Classification

UNCLASSIFIED

Security Classification

14. KEY WORDS	LINK A		LINK B		LINK C	
	ROLE	WT	ROLE	WT	ROLE	WT
Parameters	8					
Impact	6					
Airdrop operations	6					
Structures	7					
Models	7					

UNCLASSIFIED

Security Classification